Supprting Information

Triple-chromic (Photo-, Thermo-, and Mechano-chromism) of Metal Complexes Containing *N*-Salicylideneaminopyridine Ligands

Haruki Sugiyama[1,2], Atsuko Arita[1], Akiko Sekine[1], and Hidehiro Uekusa[1]*

1. Department of Chemistry, School of Science, Institute of Science Tokyo, 2-12-1, Ookayama, Meguro, Tokyo 152-8551, Japan. E-mail: uekusa@chem.sci.isct.ac.jp

2. Neutron Industrial Application Promotion Center, Comprehensive Research Organization for Science and Society, Tokai, Ibaraki, 319-1106, Japan. E-mail: h_sugiyama@cross.or.jp

Table of Contents

Figure

Table

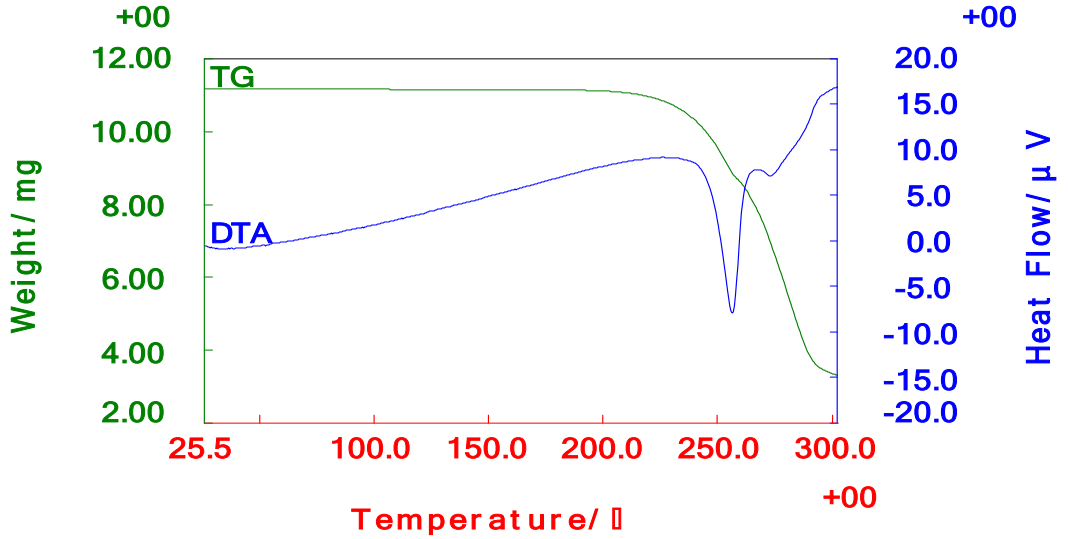

Figure S1 TG-DTA analysis of **Ni1** crystals at a rate of 5 °C/min under a dry nitrogen atmosphere (flow rate = 100 mL/min). TG analysis indicates that the **Ni1** crystal does not contain any solvent molecules, despite the presence of a minor void space within its crystal structure.

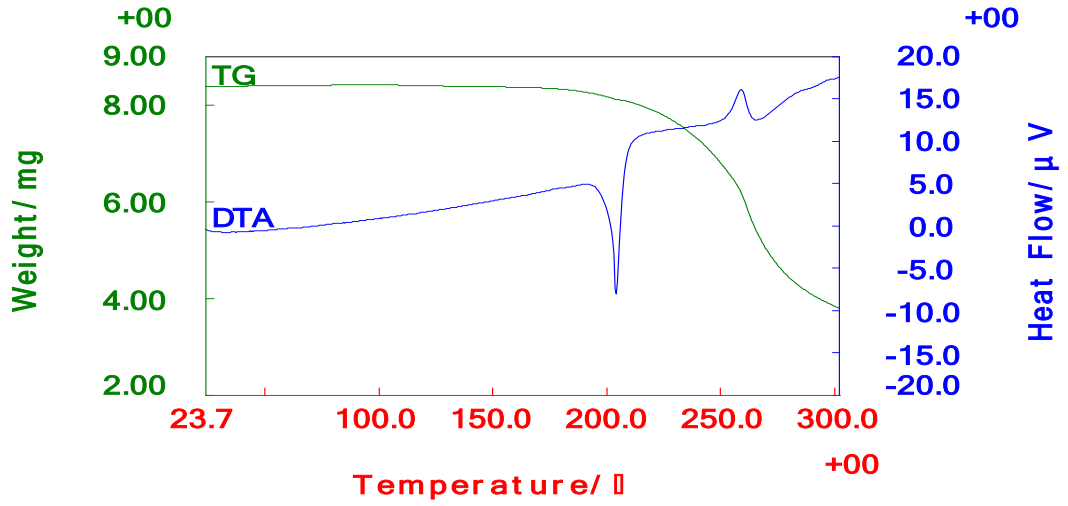

Figure S2 TG-DTA analysis of **Co1** crystal at a rate of 5 °C/min under a dry nitrogen atmosphere (flow rate = 100 mL/min). TG analysis indicates that the **Co1** crystal does not contain any solvent molecules, despite the presence of a minor void space within its crystal structure.

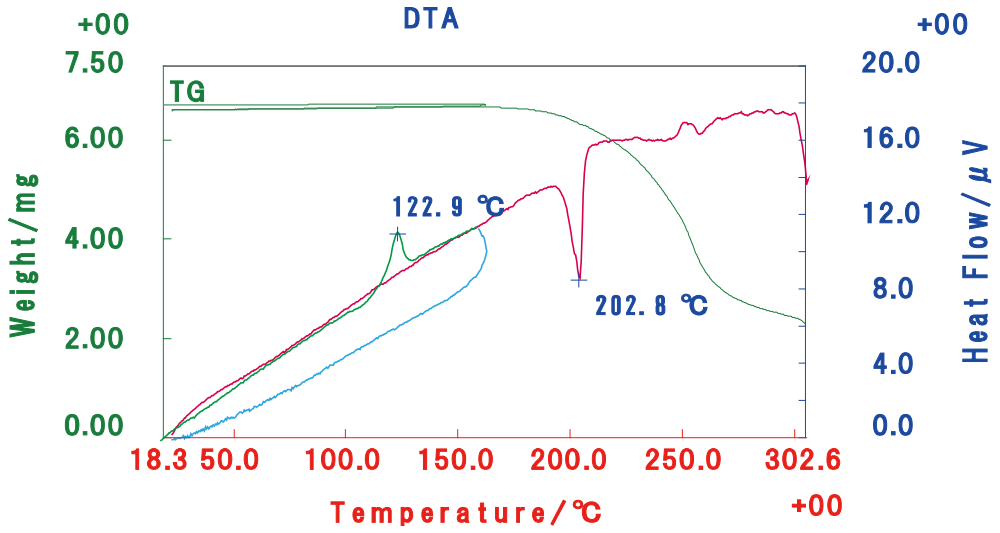

Figure.S3 TG-DTA analysis of the green amorphous phase. DTA curves were highlighted by different colors as the measurement steps. In the initial step, the temperature increased to the 150 °C (represent by green). The second step shows a temperature decrease to 20 °C (blue). Finally, the third step show a temperature increase to 310 °C (red).

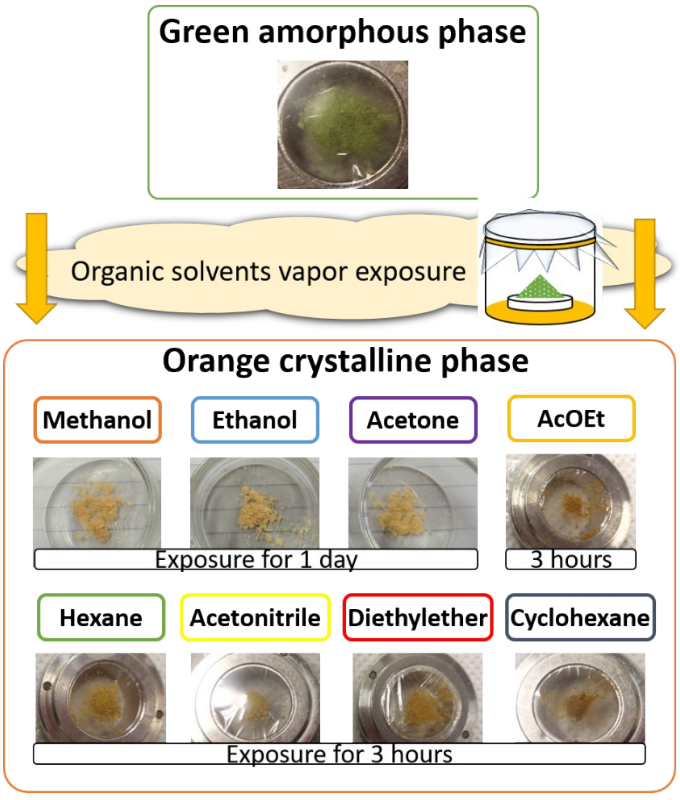

p

Figure S4 The green amorphous phase of **Co1** returned its color to orange crystalline phase upon exposure to various organic solvent vapor, such as methanol, ethanol, acetone, ethyl acetate, hexene, acetonitrile, diethyl ether, and cyclo-hexane.

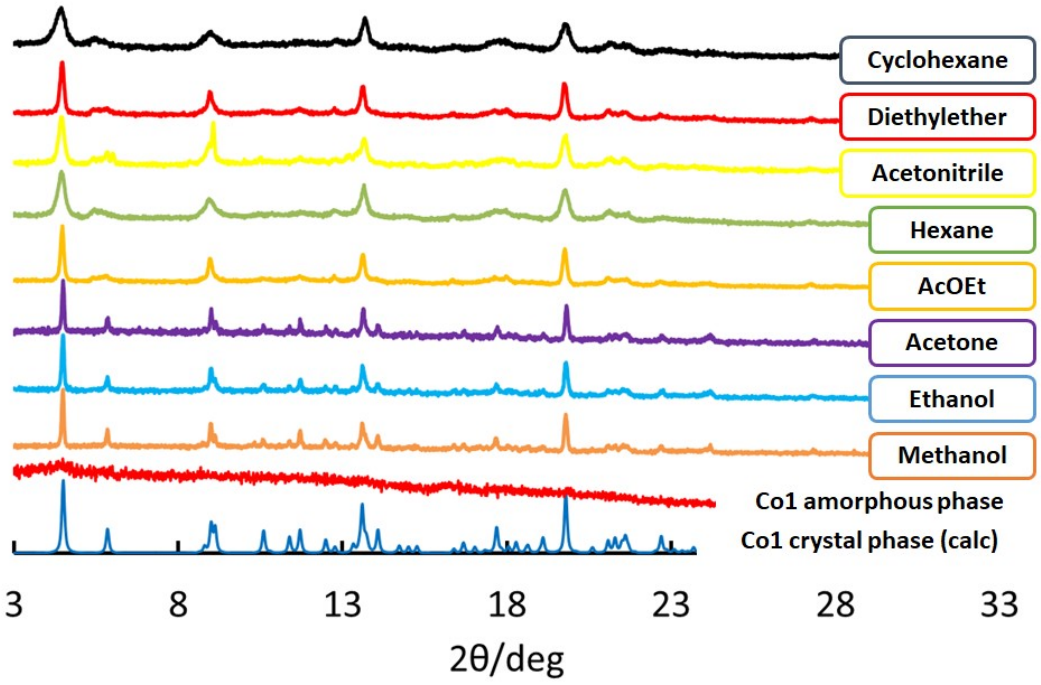

Figure S5 PXRD patterns of amorphous phase of **Co1** and emerging crystalline phases following exposure to various organic solvent vapors. The green amorphous phase of **Co1** transform to original crystalline phase upon exposure to the vapors.

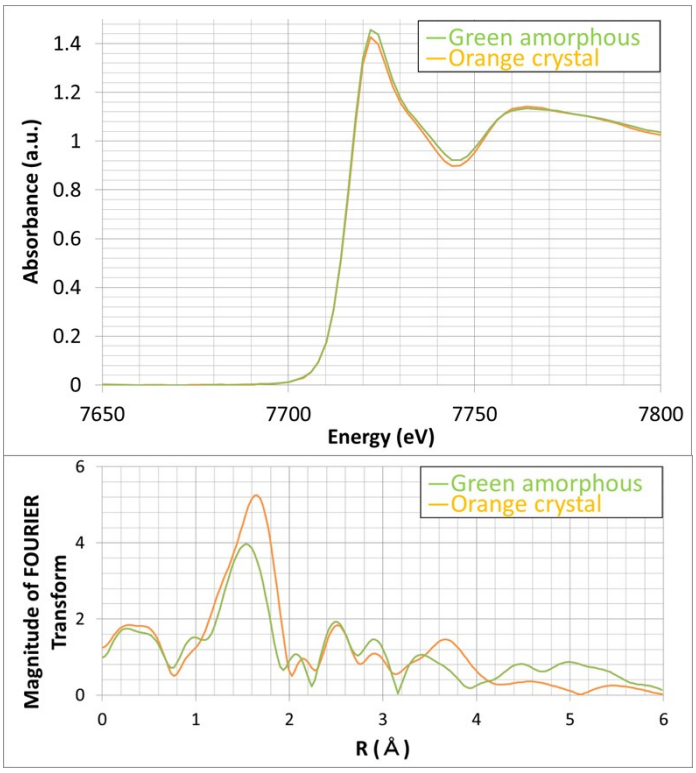

Figure S6 (a) Co K-edge X-ray absorption spectra of **Co1** crystal and amorphous. (b) The results of the Fourier transformation of the XAFS spectra.

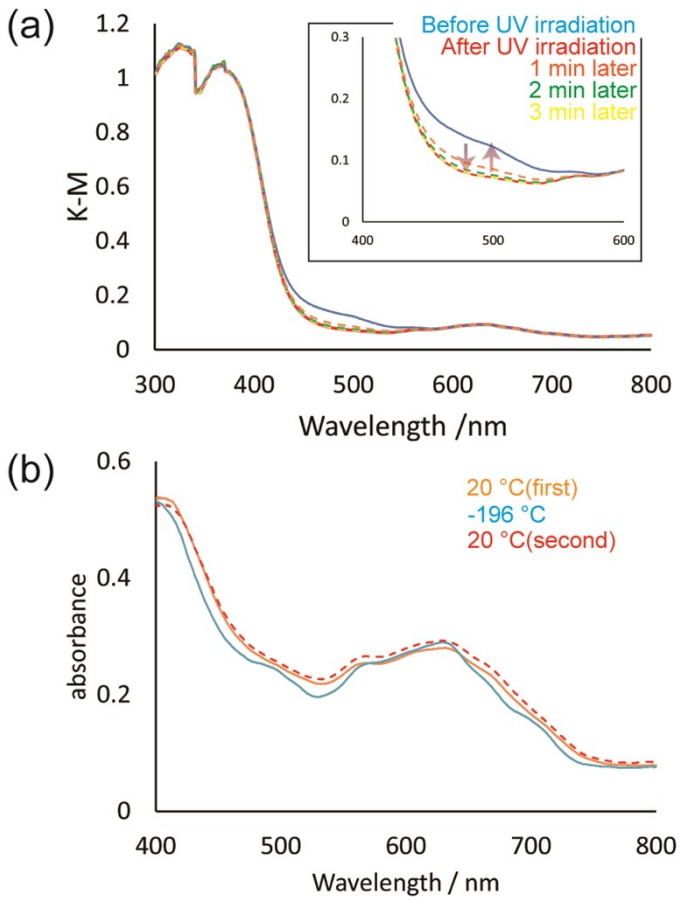

Figure S7 (a) UV-vis. spectra of **Co1** amorphous before and after UV irradiation. The absorbance at 400-450 nm was slightly increased upon UV light irradiation, and gradually decreased under visible light irradiation (550 nm). (b) UV-vis. spectra of **Co1** amorphous for the temperature change from 20 °C to -196 °C to 20 °C.

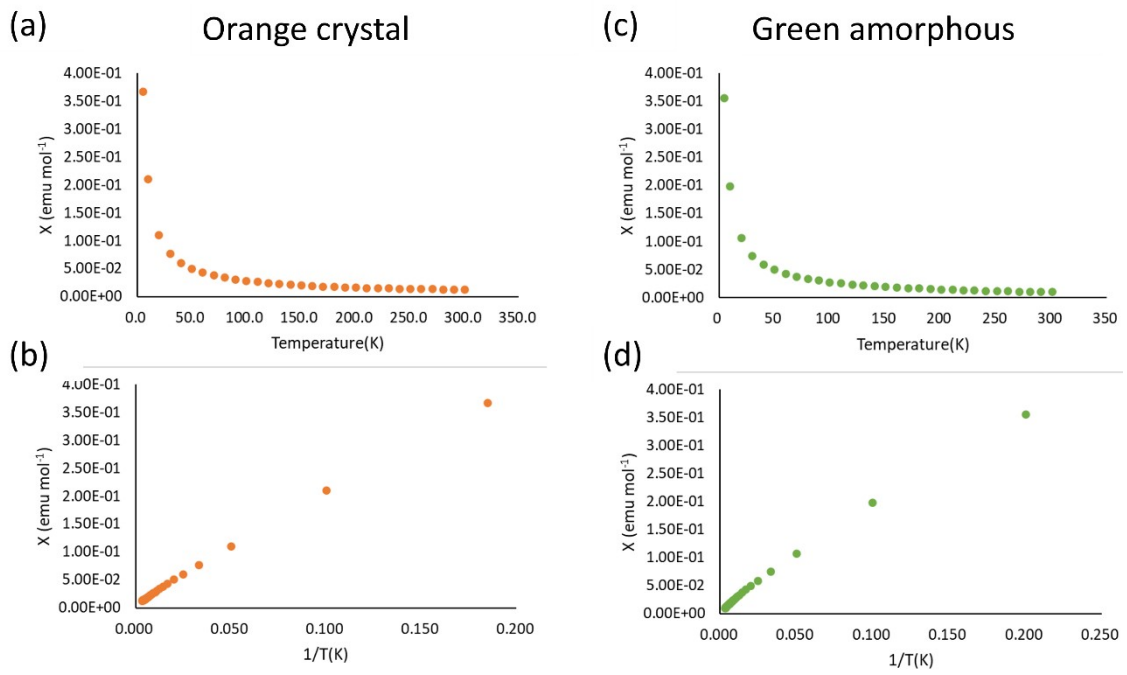

Figure S8 Temperature dependence of χ for orange crystalline phase (a, b) and green amorphous phase (c, d) at 10000 Oe from 5K to 300K. The sample information and analysis result were sumerized in Table S8.

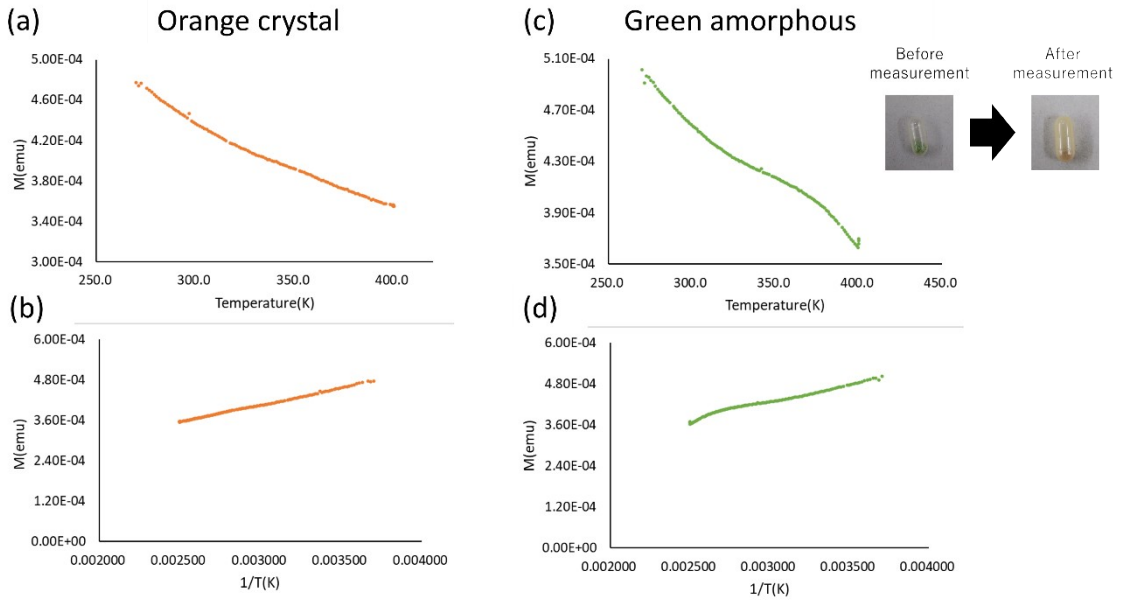

Figure S9 Temperature dependence of magnetic moment (M) for orange crystalline phase (a, b) and green amorphous phase (c, d) at 10000 Oe from 270K to 400K. The sample information and analysis result were sumerized in Table S9. For the green amorphous, the color changed from green to orange after the SQUID measurement (inserted picutres).

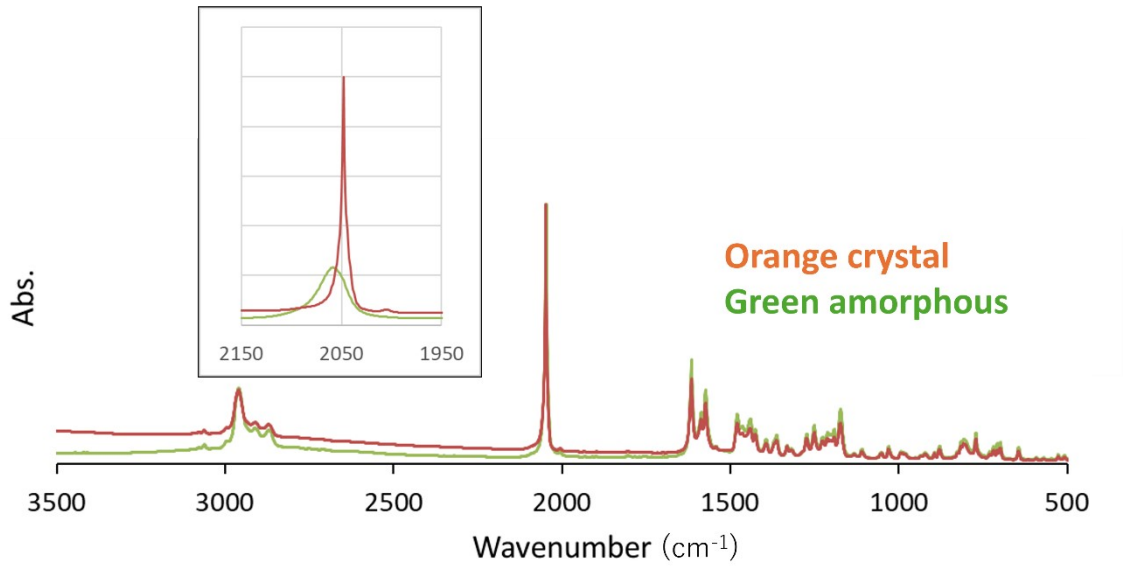

Figure S10 Infrared (IR) spectra for orange crystalline phase and green amorphous phase using a KBr disk method.

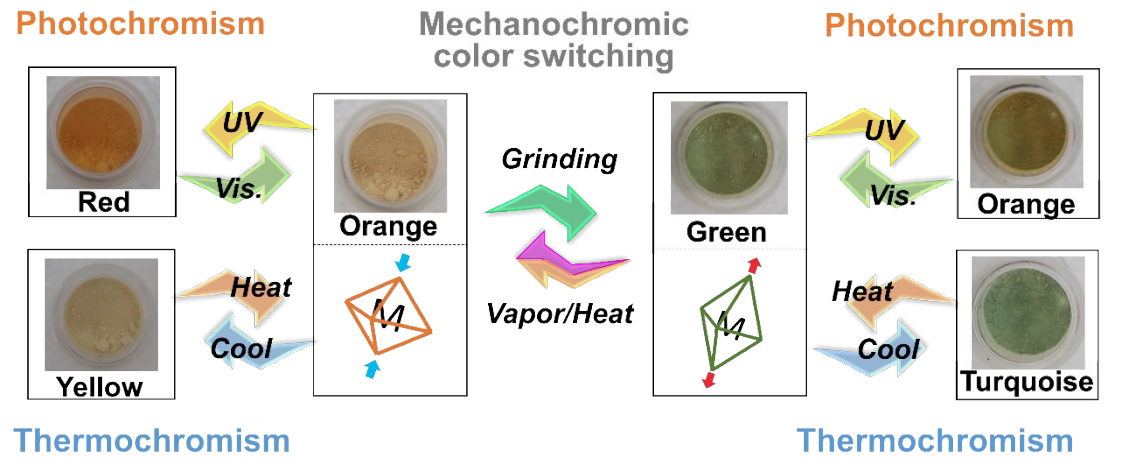

Figure S11 Summary of the chromic colour change of **Co1** crystal. The colour tones in the photochromism and thermochromism are modified by mechanochromism.

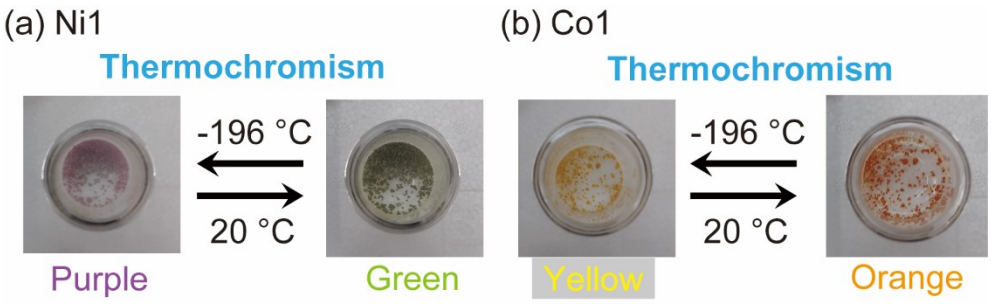

Figure S12 Thermochromic colour change of **Co1** and **Ni1** single crystals

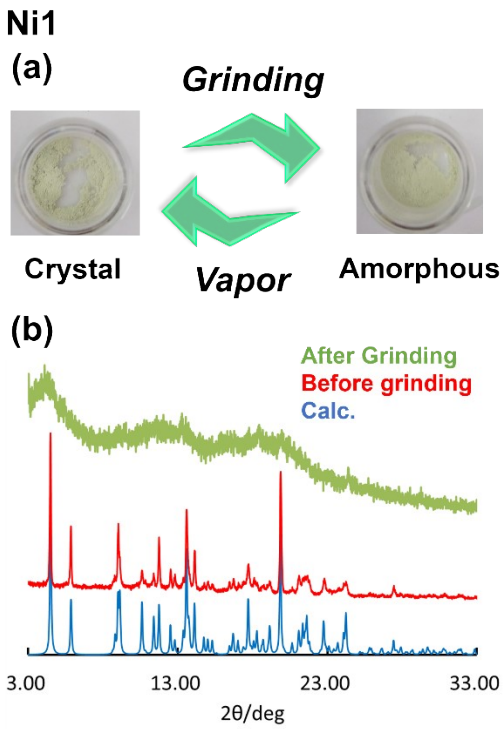

Figure S13 Sample color (a) and PXRD (b) change of **Ni1** crystals before and after grinding. Although **Ni1** crystals transformed to amorphous upon grinding, and recovered to crystalline phase by exposure in methanol vapor, the sample color did not changed through the transformation.

Table S1 Details of crystallographic data.

Identification code	**Ni1**		**Co1**	
Chemical formula	$C_{82}H_{104}N_{10}NiO_4S_2$		$C_{82}H_{104}CoN_{10}O_4S_2$	
Formula weight	1416.58		1416.80	
Temp/°C	20(2)	-180(2)	20(2)	-180(2)
wavelength/Å	1.54186		0.71075	1.54186
crystal system	Monoclinic		Monoclinic	
space group	*C*2/*c*		*C*2/*c*	
a / Å	39.408(3)	39.1141(7)	39.4956(16)	39.2182(10)
b / Å	16.3007(11)	16.0970(3)	16.3855(8)	16.1188(3)
c / Å	13.0803(8)	12.9490(2)	13.0852(7)	12.9084(2)
β / deg	95.388(3)	95.1466(8)	95.4017(15)	95.216(2)
Vol / Å^3	8365.4(9)	8120.1(2)	8430.5(7)	8126.3(3)
Z/*Z'*	4/0.5		4/0.5	
density (calculated)/ g·cm^{-3}	1.125	1.159	1.116	1.158
F(000)	3032		3028	
crystal size / mm^3	0.221 x 0.100 x 0.021		0.11 x 0.06 x 0.05	0.14 × 0.14 × 0.05
θ range for data collection	4.334 to 68.241	2.970 to 68.215	3.065 to 27.410	5.932 to 152.344
index ranges	-47 ≤ *h* ≤ 45	-46<=h<=47	-48 ≤ *h* ≤ 51	-49 ≤ h ≤ 48
	-19 ≤ *k* ≤ 17	-19<=k<=16	-21 ≤ *k* ≤ 21	-20 ≤ k ≤ 19
	-15 ≤ *l* ≤ 15	-15<=l<=15	-16 ≤ *l* ≤ 15	-15 ≤ l ≤ 12
reflections collected	38528	37109	40664	27828
independent reflections	7638	7390	9571	8259
R_{int}	0.0710	0.0696	0.0962	0.0266
absorption correction	Semi-empirical from equivalents			
max and min transmission	0.959 and 0.843	0.975 and 0.706	0.985 and 0.54	0.883 and 0.540
refinement method	Full-matrix least-squares on F^2			
data / restraints / params	7638 / 5 / 461	7390 / 3 / 459	9571 / 0 / 511	8259/0/459
goodness-of-fit on F^2	0.950	1.077	1.025	1.041
final *R* indices [$I > 2\sigma(I)$]	R_1 = 0.0575	R_1 = 0.0629	R_1 = 0.0545	R_1 = 0.0460
	wR_2 = 0.1537	wR_2 = 0.1610	wR_2 = 0.1232	wR_2 = 0.1155
R indices (all data)	R_1 = 0.0795	R_1 = 0.0789	R_1 = 0.1063	R_1 = 0.0477
	wR_2 = 0.1680	wR_2 = 0.1702	wR_2 = 0.1501	wR_2 = 0.1166
largest diff peak, hole, e·Å^{-3}	0.50 and -0.31	0.82 and -0.61	0.35 and -0.35	1.00 and -0.71
CCDC Number	2045507	2045508	2045509	2056772

Table S2 Coordination bond length and angles of **Ni1** from the X-ray structure analysis at 20 °C.

Ni1 (20 °C)			
Ni(1)-N(1)	2.053(2) Å	N(1)-Ni(1)-N(5)$^{\#1}$	90.14(8)°
Ni(1)-N(4)	2.143(2) Å	N(1)-Ni(1)-N(5)	90.43(8)°
Ni(1)-N(5)	2.116(2) Å	N(1)-Ni(1)-N(4)$^{\#1}$	89.67(7)°
		N(1)-Ni(1)-N(4)	89.76(7)°
Distortion index [5] (bond length)	0.016	N(5)-Ni(1)-N(4)$^{\#1}$	92.30(8)°
Quadratic elongation	1.001	N(5)-Ni(1)-N(5)$^{\#1}$	88.93(11)°
#1: -x+1, y, -z+1/2			

Table S3 Coordination bond length and angles of **Ni1** from the X-ray structure analysis at -180 °C

Ni1 (-180 °C)			
Ni(1)-N(1)	2.061(2) Å	N(1)-Ni(1)-N(5)$^{\#1}$	89.73(8)°
Ni(1)-N(4)	2.122(2) Å	N(1)-Ni(1)-N(5)	90.86(8)°
Ni(1)-N(5)	2.110(2) Å	N(1)-Ni(1)-N(4)$^{\#1}$	89.54(8)°
		N(1)-Ni(1)-N(4)	89.85(8)°
Distortion index (bond length)	0.012	N(5)-Ni(1)-N(4)$^{\#1}$	92.28(8)°
Quadratic elongation	1.001	N(5)-Ni(1)-N(5)$^{\#1}$	88.70(10)°
#1: -x+1, y, -z+1/2			

Table S4 Coordination bond length and angles of **Co1** at 20 °C

Co1 (20 °C)			
Co(1)-N(1)	2.078(2) Å	N(1)-Co(1)-N(5)$^{\#1}$	90.17(8)°
Co(1)-N(5)	2.173(2) Å	N(1)-Co(1)-N(5)	90.74(7)°
Co(1)-N(4)	2.197(2) Å	N(1)-Co(1)-N(4)$^{\#1}$	89.46(8)°
		N(1)-Co(1)-N(4)	89.60(7)°
Distortion index (bond length)	0.022	N(5)-Co(1)-N(4)$^{\#1}$	92.71(7)°
Quadratic elongation	1.002	N(5)-Co(1)-N(5)$^{\#1}$	88.55(10)°
#1: -x+1, y, -z+1/2			

Table S5 Coordination bond length and angles of **Co1** from the X-ray structure analysis at -180 °C

Co1 (-180 °C)			
Co(1)-N(1)	2.079(1) Å	N(1)-Co(1)-N(5)$^{\#1}$	90.21(6)°
Co(1)-N(5)	2.154(2) Å	N(1)-Co(1)-N(5)	89.81(6)°
Co(1)-N(4)	2.174(2) Å	N(1)-Co(1)-N(4)$^{\#1}$	89.30(6)°
		N(1)-Co(1)-N(4)	89.66(6)°
Distortion index (bond length)	0.018	N(5)-Co(1)-N(4)$^{\#1}$	92.77(6)°
Quadratic elongation	1.002	N(5)-Co(1)-N(5)$^{\#1}$	88.25(8)°
#1: -x+1, y, -z+1/2			

Table S6 Local structure parameters of N shells around the Co(II) ion in the **Co1** amorphous. Parameters of R were estimated by fitting. Parameters with (*) were fixed.

	N	R	dE	DW	MF
＜2 shell＞	4.0 *	2.066 Å	1.59 *	0.08 *	4.0 *
Octahedral	2.0 *	2.238 Å			

Table S7 Coordination bond lengths of the **Co1** complex in the crystal and amorphous phases estimated by SXRD and XAFS analysis at room temperature.

Bond length	Crystal Phase [SXRD]	Bond length [XAFS]
Co…N_{SAP1}	2.197(2) Å	2.066 Å
Co…N_{SAP2}	2.173(2) Å	
Co…N_{NCS}	2.078(2) Å	2.238 Å

Table S8 The sample information and analysis result of magnetic magnetic investigation investigation was carried out from 5K-300K

Name	Orange crystal	Green amorphous
Sample weight (mg)	3.04	8.58
curie constant (emu K mol^{-1})	1.98	1.79
μ_{eff}	3.97	3.78
$2\sqrt{S(S+1)}$ (S=3/2)	3.872983346	3.87

Table S9 The sample information and analysis result of magnetic magnetic investigation investigation was carried out from 270K-400K

Name	Orange crystal	Green amorphous
Sample weight (mg)	6.16	6.34
χ(emu mol^{-1}) at 293K	0.0102	0.0104